Fall 2019

Developing a model system of liquid lubricants for space applications: Multiple alkylated cyclopentane in alumina enclosed surface

Vidit Singh

Department:

DEVELOPING A MODEL SYSTEM OF LIQUID LUBRICANTS FOR SPACE APPLICATIONS: MULTIPLE ALKYLATED CYCLOPENTANE IN ALUMINA ENCLOSED SURFACE

by

VIDIT SINGH

A THESIS

Presented to the Faculty of the Graduate School of the

MISSOURI UNIVERSITY OF SCIENCE AND TECHNOLOGY

In Partial Fulfillment of the Requirements for the Degree

MASTER OF SCIENCE IN CHEMICAL ENGINEERING

2019

Approved by:

Dr. Jee-Ching Wang, Advisor
Dr. P. Neogi
Dr. Dipak Barua

ABSTRACT

Lubricants are substances used for reducing friction wear tear and energy losses between two moving bodies. For space applications, normal lubricants cannot be used as they cannot survive the harsh and demanding conditions of space. Multiple Alkylated Cyclopentanes (MACs) have been utilized as space lubricants in recent times with tremendous results. NASA uses the MACs for their missions in space, in particular 1,3,4-tri-(2-octyldodecyl) cyclopentane sold by Nye Lubricants under the name of Pennzane™.

In this research, an effort has been made to identify appropriate potential models for simulating Pennzane molecules and to develop MD simulation codes to construct realistic model systems comprising Pennzane thin films sandwiched between two α-alumina surfaces. The results from the MD simulations show that, unlike symmetric molecules that can be induced by nanoscopic confinement to form layered configurations, the highly branched Pennzane possesses sufficient structural asymmetry and complexity to resist the layering tendency. Surface interactions are found to bend segments of the proximal branches into non-trans conformations that lie parallel to the surfaces. The resultant strong interactions appear to function as an anchor that promotes the branches in a crowded environment to stand more straight up.

The realistic model system of an important liquid lubricant developed in this work can serve as a key to open many research directions and possibilities, including the effects of inorganic lubricant additives such as graphene and organic lubricant additives such as tri-(2-octyldodecyl) phosphate to be investigated by rigorous MD modeling and simulation studies.

ACKNOWLEDGMENTS

First and the foremost, I would like to thank my thesis advisor, Dr. Jee-Ching Wang, of the Chemical and Biochemical Engineering Department at Missouri University of Science and Technology, Rolla. Dr. Wang's office door was never closed for me whenever I had a question about my research, writing, or any personal problem. He gave me enough time to think about it, make steady and stable progress and kept steering me in the right direction.

Secondly, I would also like to thank the adjudicators/committee members, who were deeply involved in the validation process of this research project: Dr. Parthasakha Neogi and Dr. Dipak Barua. It would have been difficult to successfully complete this validation of project without their input and valuable suggestions.

Finally, I express my deep gratitude to my family, friends and my girlfriend for providing me with undeterred support and continuous moral uplifting throughout my time of research and through the process of writing this thesis. It would not have been possible without their encouragement.

Thank you.

TABLE OF CONTENTS

Page

LIST OF ILLUSTRATIONS

LIST OF TABLES

1. INTRODUCTION

1.1. BACKGROUND

Historically, space lubricants have not been chosen according to the latest technology or the best materials available to scientists because of the limited duration of the specific intention of the mission. As time progressed, the length of time and the expectation from the spacecraft and the mission increased. The spacecraft needed to be more sophisticated and had to stay for a longer time in the harsh conditions outside the earth's atmosphere. This called for the abatement of the mechanical failures caused by the parts that had to stay longer in difficult and fluctuating conditions of heat, pressure, and space radiation. Fundamental aspects, including rheology of space lubricants, were brought into focus and put to the test only when the scientists detected and attempted to solve the issue related to mechanical failures. However, since the last three decades, space lubricants properties have greatly improved and hence the mission's chances of survival due to reduced mechanical failures.

The main purpose of applying lubricants is to separate the surfaces in motion with respect to each other (relative motion). It creates an environment where there are low friction and low shear resistance. Lubricants reduce the cost of operational maintenance and material damage. The proper type of lubricants is decided to depend upon the load, shear stress, and temperature of a specific job. In general, there are three categories of lubricants: solid, liquid, and mixed regime lubricants, and the proper choice is according to the job requirements. This research is concerned with the liquid lubricants suitable for space engineering applications.

In the last 30 years, a lot of different liquid lubricants, including silicones, polyphenyl ethers, mineral oils, perfluoro polyether, and esters, have been tested extensively to see which one the best of the lot is for space engineering. The most effective one appears to have been a recently developed synthetic hydrocarbon called Pennzane™ [1-4], which has been replacing conventional choices because of its better adaptability in the conditions of the space environment. Pennzane belongs to a class of hydrocarbon called MACs (Multiple Alkylated Cyclopentanes) that are synthesized by reacting cyclopentadiene in alkaline conditions and then taken through hydrogenation process to obtain the ultimate product: a mixture of multiple alkylated cyclopentane (dialkylated-, trialkylated-, Pentaalkylated-, etc.). The ratios of the different alkylations can be varied by changing the reaction conditions during their formation. NASA has been using Pennzane™ sold by Nye Lubricants under the name of SHF-X2000 (marked as Nye Lubricant 2001A) [1-4] whose chemical formula is tri-2-octyldodecyl substituted cyclopentane. NASA has performed an extensive test for six years to examine and verify the results of the lubricant.

1.2. PROPERTIES OF MULTIPLE ALKYLATED CYCLOPENTANES (MACs)

A good lubricant must have certain chemical and physical properties to work in a proper manner when in mechanical contact with moving parts during operation. In the case of space applications, suitable lubricants are particularly evaluated in the following aspects:

1.2.1. Wearability. Lubricants are added between the moving surfaces to prevent direct contact between the surfaces. If the moving surfaces come in direct contact, there

will be a lot of friction which in turn would create wear and tear as well as huge energy losses apart from damage to the devices. As an easy solution to prevent or reduce these problems, lubricants ideally provide both a slip condition for the moving surfaces and cushioning between the surfaces. Although no lubricant is ideal, MACs stand out by possessing a lower friction coefficient factor, assess at 0.12, that makes the surfaces less wearable as compared to other traditional lubricants on the moving surfaces. Friction and wear properties of MACs have been measured using 4 ball Wear test by Zhang et al. [4] Another method to measure the frictional properties is SVG analysis [5] as mentioned by Nye Lubricants on their website. Additional relevant properties of MACs are summarized in Table 1.1. [1-4]

Table 1.1. Physical Properties of MACs

Lubricant	**Mol. Weight**	**Kinematic Viscosity at 100°C (cSt)**	**Viscosity Index**	**Surface Tension (mN m^{-1})**	**Vapor Pressure at 20°C (torr)**
MACs	910	9.3	148	24.5	5.6×10^{-6}

1.2.2. Stability in the Vacuum. Although certain mechanical seals (such as labyrinth seal) are used in space mechanisms to provide a tortuous path to prevent lubricant loss, it is still a potential problem faced by missions that require spacecraft to be in space conditions for a long period of time. [2,3,5] Lubricant loss at exit area and at a fixed temperature is proportional to the vapor pressure of the lubricant. As compared to conventional lubricants, Pennzane™ is a particularly good candidate with a similar range of viscosity.

1.2.3. Reduced Creeping Tendency. Creeping is a property of a liquid, to migrate over the moving mechanical surfaces, which is inversely related to the surface tension of the liquid in question. Fluids used as lubricants in recent time like PTFE (Polytetrafluoroethylene), MACs, silicones, esters, and hydrocarbons have a lesser tendency to creep over the mechanical parts as compared to more traditional lubricant fluids. Also, these traditional fluids are inclined to render the barrier films corroded and useless after a long period of contact time, hence less effective as lubricant fluids. [2,3,5,6] In this respect, Pennzane™ lubricant has been shown to have higher surface tension and a lower creeping tendency, thereby a better choice than the traditional lubricant fluids.

1.2.4. Viscosity-Temperature Properties. Occasionally, low temperatures (14°F to -4°F) are encountered in space applications where traditional lubricants may become undesirable because they become viscous and their pour point increases. [1-6] Lubricants such as Pennzane that retain reasonable viscosities at low temperatures are ideal for space applications.

1.2.5. Elastohydrodynamic Properties. The physics behind the lubrication is that when a lubricant is passed in between the moving surfaces, it forms a thin layer where the moving surfaces get into a slip, at the surface of the thin layer formed. This thin layer is called an elastohydrodynamic (EHL) film. Two essential physical properties that influence the functions of a thin layer EHL film are pressure-viscosity coefficient and viscosity. [1,2,6] While the factors affecting viscosity are chemical structure influence and molecular viscosity, the pressure-viscosity coefficient is only related to chemical structure, except when the molecular weight of the lubricant is low.

1.2.6. Boundary Lubrication Properties. Boundary lubrication is the lubrication regime where the spacing between two solid surfaces becomes too small, and the lubricant film in between becomes too thin so that there is a possibility for the two opposing solid surfaces, more specifically their asperities, to come in contact with each other. This can also exert great stress on the lubricant molecules to cause their molecular structures to break. To avoid exactly this contact between the two opposing asperities is the most important aspect of boundary lubrication. Understandably, the chemistry of the lubricant film, roughness of the solid and the surface separation surfaces determine the occurrence and severity of boundary lubrication. It can be considered that when the thickness of the protective lubricant film is down to a few nanometers, even nominally smooth surfaces may encounter boundary lubrication. [1,2,4,6] Pennzane^{TM} has a very stable structure and hence a very slow progression toward failure and a longer lubricated lifetime as compared to traditional lubricating fluids.

Boundary lubrication properties can also be improved by the selection of appropriate materials for the balls, in ball bearing and gear teeth, in the gear box. [1-3] But, the material selection of the surfaces in contact is beyond this research scope.

1.3. GRAPHENE ADDITIVE

Due to our ambitious and curious nature, humanity has been driving to explore ways to improve the qualities of lubricants. An important way that has been commonly practiced for increasing the wearability and enhancing other tribological properties of lubricants is to add additives. Graphene is a 2-D carbon material whose stable structure was isolated in the early 2000s. It has pulled a lot of attention in various fields of

application. Amongst these fields, the tribological behavior of graphene additive has been relatively less studied. [7] It is thus of significant scientific interest and practical importance to study the tribological behavior of a Pennzane-graphene composite lubricant system. Although the addition of graphene as a lubricant additive is outside of the scope of this research, which is focused on developing a realistic model system for the molecular dynamics (MD) simulation studies of nanoscopically confined Pennzane films, it is considered relevant and beneficial to highlight graphene's unusual properties, in particular those that help reduce wear and friction and lead to an enhanced lubrication system applicable in the spacecraft.

In recent years, graphene has established itself as a valuable asset in the optical, mechanical, thermal, and electrical application. [7,8] It has high mechanical strength which can be tested using an isolated sheet of graphene and an Atomic Force Microscopy (AFM) probe with a diamond tip to analyze the graphene's breaking strength. The Young's modulus of graphene film was found to be equal to 1 Tera-Pascal.[7,8] Also, it's been proven quite recently that the overall strength is not owed to the grain boundaries, even though other kinds of defects, including those caused by oxidation, reduces the mechanical properties of graphene (strength and stiffness). [8] Such outstanding strength is greatly beneficial to the protection of surfaces from wear and tear as demonstrated by the studies of Lee *et al*. [9] Moreover, graphene has been found to be leakproof to gases and other fluids, thereby diminishing the oxidation and corrosion factors that commonly cause damage to surface in contact.

Graphene is a material with extremely low surface energy and with multiple smooth layers stacked together via relatively weak physical interactions that allow the

graphene layers to slide past each other relatively easily. Its small thickness and size can also fit into and fill many corrugations on solid surfaces, hence capable of assisting a broad range of contacts to reduce frictional losses and wearability. [10] These properties make graphene suitable as a solid lubricant itself as compared to other carefully synthesized thin solid lubricant films. They also make graphene very lucrative for ever-improving mechanical applications to achieve reduced wear and tear systems.

Graphene can also be used as a colloidal dispersion in oil-based nonpolar liquid lubricants. Its unique smooth surface and closely packed structure can impart high strength and low shear capabilities into the lubricant in addition to its impressive chemical inertness. It is particularly suited for systems like [8,9-11] nanoelectromechanical (NEMS) and microelectromechanical systems (MEMS) due to its thinness even though multiple layered.

1.3.1. Manufacturing. Graphene's property depends upon the diameter of individual particles (grains), thickness, pattern, and how crammed up are the defects formed during its manufacturing process. The first successful attempt to produce graphene on a routine basis was by mechanical exfoliation where sticky tapes were used to remove sheets from highly ordered pyrolytic graphite (HOPG), transferred thereafter by gluing the sticky-tape onto the final object and then pulling the tape out. [7,9,11] Since then a number of methods have been devised to produce graphene, including dry mechanical or chemical exfoliation and reverse rolling of carbon nanotubes (CNTs) by electrochemical, chemical, or physical means. Additionally, chemical vapor deposition, electric breakdown of gases, and reduced graphene oxide have also been employed. For

example, graphene of high purity can be made by chemical vapor deposition on surfaces of nickel or copper metals, in the presence of hydrocarbon vapors.

1.3.2. Utility of Graphene. Graphene has shown promising results when used in some solid lubricants. [7,9-11] It was demonstrated that when 10% of graphene platelets were added as Nano-filters to the solid lubricant, the wearing went down by 10^{-4}. It is also widely known in recent times that the addition of graphene even in really small amounts to lubrication fluids can drastically lessen friction and wear of steel. Tests were carried out on a 4-ball wear apparatus (1200 rpm, 147 N, 75°C) on graphene spread in oil by physical means.[7,9,11] The results showed that graphene at 0.075% by weight could improve the load-bearing capability of the oil or oil doped with graphene. Furthermore, the frictional force was found to decrease when the base oil was improved with graphene. [8,9,11,12] In other experimental studies, alkylated graphene with varying alkyl chain groups and carboxylic groups were dispersed in various organic solvents. Results from tribological tests confirmed that, when hexadecane was introduced with graphene, the friction of steel was reduced by 26%. Although such improvements have been attributed to the smoothened surfaces and minimized the connection between the provided surfaces due to the continuous presence of graphene, the complete physics behind is still not fully understood and may include the effects of graphene on the conformations and configurations of the lubricant molecules.

1.4. OBJECTIVES

The prime objective of the research is: developing a molecular-based physical representation of Pennzane thin film in a representative tribological environment and then

construct a realistic model system to be employed in MD modeling and simulation studies aimed at providing lubrication support for space applications. In order to meet the harsh conditions of space engineering, the surfaces are usually hard anodized with aluminum or aluminum alloys to reduce [13] the surface wear and tear. The detonation sprayed aluminum coatings on an unlubricated sliding have shown a marked reduction in wear behavior, with a friction factor of 0.4-0.5. [14] A hard anodized aluminum is basically an electrochemical process in which the aluminum is electroplated on a metal surface (e.g., steel) where aluminum naturally forms an oxide, that is, alumina. The hard anodized aluminum oxide thus formed is uniform, dense, and harder when compared with natural oxidation.

In addition to improved lubrication, there are other potential benefits from hard anodizing. The surfaces are easier to clean and give a better aesthetic appearance and better resistance to peeling, flaking or chipping, abrasion, flame, and contamination. In this research, the devised model system will comprise a thin Pennzane lubricant film confined between two alumina surfaces, on a nanoscopic scale, in order to be more related to important engineering applications, including space missions.

2. METHODOLOGY

2.1. MOLECULAR DYNAMIC SIMULATION

Molecular Dynamics (MD) has been a widely employed and trusted method for simulating and studying structural and dynamic properties of various systems at a molecular scale that are generally too complicated for first-principle analytical approaches or for conventional continuum-based modeling methodologies.[15,16] The essence of MD is to numerically solve *N*-particle equations of Newtonian classical mechanics for a model system constructed by the *N* particles. In general, the equation of motion for a given particle *i* can be expressed as

$$m\ddot{r} = f_i + g_i \tag{2.1}$$

where $\ddot{r}$ and *m* are the instantaneous acceleration and the mass of the particle, whereas $\mathbf{f}_i$ and $\mathbf{g}_i$ represent the net interaction force and the net constraint force on the particle. For clarification, Eq. (2.1) can also be converted into two first-order differential equations as follows,

$$\dot{p} = f_i + \chi p_i \tag{2.2a}$$

$$m_i\dot{r}_i = p_i \tag{2.2b}$$

where **p** is the momentum of particle *i*, $\dot{\mathbf{p}}$ is the rate of change of momentum, $\dot{\mathbf{r}}$ is the velocity, and χ is the system-wide coefficients for representing the imposed constraints. In this project, the constituent molecules face a geometric constraint that confines the molecules to form a nano-thin lubricant film and a thermal constraint that controls the system temperature as room temperature at all times. While the geometric constraint will

be represented by explicit atoms, the thermal constraint is represented by a "friction" coefficient evaluated instantaneously by the following method,

$$\frac{dT}{dt}=\frac{d}{dt}\left(\frac{1}{3k_B n_{dof}}\sum_{i=1}^{N}\frac{\mathbf{p}_i^2}{m_i}\right)\propto\sum_{i=1}^{N}\mathbf{p}_i\cdot\dot{\mathbf{p}}_i=0\ , \tag{2.3}$$

where k_B is the Boltzmann constant and n_{dof} is the total number of degrees of freedom. After substituting the equation of motion, Eq. (2.1), into the above Eq. (2.4), the resulting expression for the friction coefficient becomes

$$\chi=-\frac{\sum_{i=1}^{N}\mathbf{p}_i\mathbf{f}_i}{\sum_{i=1}^{N}|\mathbf{p}_i|^2}\ . \tag{2.4}$$

Numerically speaking, the MD method as shown by Eqs. (2.1) or (2.2) is an initial-value problem. For computational efficiency and for convenient incorporation of temperature control, the Leap-frog integration algorithm is adopted in this work, which integrates the equation of motion through the following discretization and operation for velocities,

$$\mathbf{v}(t+\frac{1}{2}\Delta t)=\mathbf{v}(t)+\mathbf{a}(t)\frac{1}{2}\Delta t+\mathbf{b}(t)\left(\frac{1}{2}\Delta t\right)^2+\cdots$$

$$-\quad\mathbf{v}(t-\frac{1}{2}\Delta t)=\mathbf{v}(t)-\mathbf{a}(t)\frac{1}{2}\Delta t+\mathbf{b}(t)\left(\frac{1}{2}\Delta t\right)^2+\cdots$$

$$\Rightarrow\ \mathbf{v}\,(t+\tfrac{1}{2}\Delta t\,)=v\,(t-\tfrac{1}{2}\Delta t)+\mathbf{a}(t)\,\Delta t+\vartheta\left((\Delta t)^3\right) \tag{2.5}$$

and for coordinates,

$$\mathbf{r}(t+\Delta t)=\mathbf{r}(t+\frac{1}{2}\Delta t)+\mathbf{v}(t+\frac{1}{2}\Delta t)\frac{1}{2}\Delta t+\frac{1}{2}\mathbf{a}(t)\left(\frac{1}{2}\Delta t\right)^2+\frac{1}{6}\mathbf{b}(t)\left(\frac{1}{2}\Delta t\right)^3+\cdots$$

$$-\qquad\mathbf{r}(t)=\mathbf{r}(t+\frac{1}{2}\Delta t)-v(t+\frac{1}{2}\Delta t)\frac{1}{2}\Delta t+\frac{1}{2}\mathbf{a}(t)\left(\frac{1}{2}\Delta t\right)^2-\frac{1}{6}\mathbf{b}(t)\left(\frac{1}{2}\Delta t\right)^3+\cdots$$

$$\Rightarrow\quad\mathbf{r}(t+\Delta t)=\mathbf{r}(t)+\mathbf{v}(t+\frac{1}{2}\Delta t)+\vartheta\left((\Delta t)^3\right) \tag{2.6}$$

where Δt is a time interval and usually around 1-2 fs (10^{-15} sec) for simulating complex molecules. Notably, the temperature control here, can be conveniently incorporated into Eq. (2.6),

$$v(t+\tfrac{1}{2}\Delta t) = v(t-\tfrac{1}{2}\Delta t) + \left(\frac{f(t)}{m}+\chi v(t)\right)\Delta t \qquad (2.7)$$

and implemented using a procedure devised by Brown and Clarke. [17]

It can be stated that, while the engine of the MD approach is played by the numerical integration algorithm, the all-important fuel is the interaction forces which are derivatives of the total interaction potential energy $U(\mathbf{r}^N)$ with respect to the particle coordinate as shown below,

$$\mathbf{f}_i = -\frac{\partial U(\mathbf{r}^N)}{\partial \mathbf{r}_i} . \qquad (2.8)$$

When applied to model systems comprising complex molecules and geometries, $U(\mathbf{r})$ itself is a complex function of all the particles' coordinates as well as of the system's geometry. From the viewpoint of the constituent molecules, $U(\mathbf{r})$ can be expressed as follows as a sum of two decoupled contributions,

$$U(\mathbf{r}) = U^{intra}(\mathbf{r}) + U^{inter}(\mathbf{r}) , \qquad (2.9)$$

where $U^{intra}(\mathbf{r})$ represents the intra-molecular interaction potential energies that are needed in order to provide and retain the chemical structure of a model molecule, and $U^{inter}(\mathbf{r})$ denotes the inter-molecular interaction potential energies due to the constituent molecules interacting with themselves and with other components in the model system. The MD modeling approach is based on a very small number of fundamental approximations and assumptions. Its validity in representing and predicting reality is dictated mostly by the potential energy models employed to construct the model system

and describe the interactions among the constituent particles. For this purpose, successful potential energy models need to consider not only accuracy but also efficiency and transferability.

2.2. MULTIPLE ALKYLATED CYCLOPENTANE STRUCTURE

The selected lubricant molecule for this project is 1,3,4-tri-(2-octyldodecyl) cyclopentane, also known commercially as Pennzane. As shown in Figure 2.1, it is a highly branched alkane that has three 2-octyldodecyl branches attached to the 1^{st}, 2^{nd} and 4^{th} carbon atoms of the core cyclopentane ring. Its chemical formula includes 6 methyl (CH_3) groups, 6 methine (CH) groups, and 53 methylene (CH_2) groups, resulting in a molecular mass equivalent to $(CH_2)_{65}$. When compared to its linear isomers, Pennzane demonstrates significantly better tribological behavior, which can certainly be attributed to its alkyl branches. Generally speaking, branched isomers of alkanes are better lubricants and better fuels than linear isomers. From a fundamental point of view, the multiple long branches of Pennzane are likely to entangle with one another between different molecules, which may be a desirable configuration underpinning excellent lubrication behavior.

Interaction Potential Models for Pennzane. In the field of molecular modeling and simulation, alkanes are typically simulated by a united atom (UA) approach where each of the methyl, methylene, and methine group is modeled as a pseudo-atom equivalent to the H atoms fused into the central C atom. This approach has evolved into a small number of variations over the years and a recent development through a series of

systematic, rigorous studies is the so-called [18-20] TraPPE (Transferable Potentials for Phase Equilibria) family of the force fields.

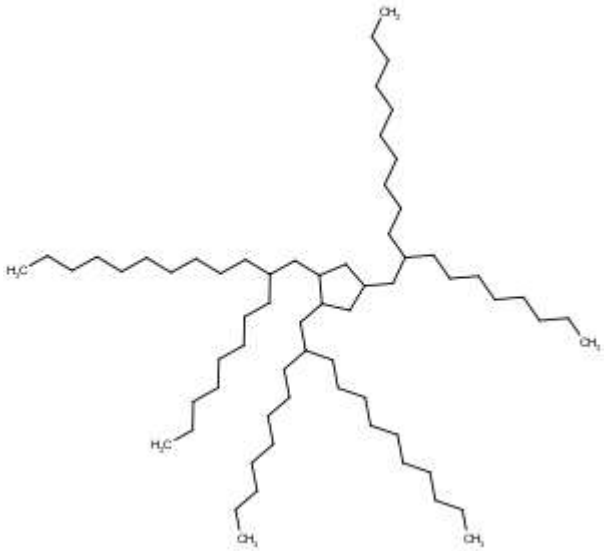

Figure 2.1. Structure of 1,3,4-tri-(2-octyldodecyl) cyclopentane

The different pseudo-atoms (UA) in Pennzane are all covered in the TraPPE force fields, which are thus adopted for this project. The resultant model Pennzane molecule is depicted in Figure 2.2 where each green bead represents a UA that is also numerically labeled in the MD simulations. In this work, the relatively fast C-C bond stretching is frozen by the SHAKE algorithm [15] and constrained to 1.54 Å [18-20] in order to allow larger time intervals (Δt) to be used. Thus, the intramolecular potential energy, U^{intra}, for Pennzane includes contributions from C-C-C-C torsional (dihedral) motions and C-C-C bond bending, as well as non-bonded dispersion interactions between UA's more than three bonds apart. Specifically, the bond bending motion is modeled by a harmonic potential,

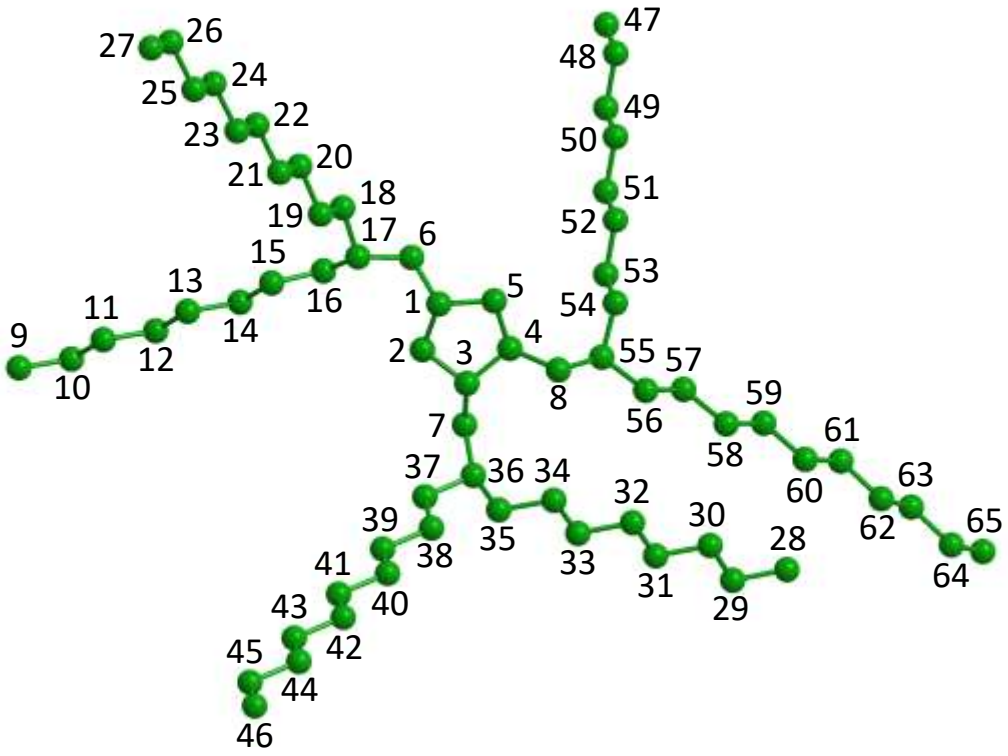

Figure 2.2. A Pennzane molecule modeled by a United-Atom Approach. The numbers are numerical labels used to identify each UA in the MD simulations.

$$U^{intra}(\mathbf{r}) = \sum_{i=3}^{n} U_b(\theta_i) + \sum_{i=4}^{n} U_t(\phi_i) + \sum_{i=1}^{n-4} \sum_{j=i+4}^{n} U_{LJ}(r_{ij}) \quad (2.10)$$

$$U_b(\theta_i) = \frac{1}{2} k_\theta (\theta_i - \theta_0)^2 \quad (2.11)$$

where θ_i is an instantaneous C-C-C bond angle and θ_0 is its equilibrium value. The value of the force constant, k_θ, [18-20] is fixed at $62500k_B$ for all bond angles in normal, branched, and cyclic alkanes. For the torsional motion, the TraPPE force fields provided two different fitted potential functions: one for normal and branched alkanes and one for cyclic alkanes, but both can be converted into the following form,

$$U_t(\phi_i)=a_0+a_1\cos\phi_i+a_2\cos(2\phi_i)+a_3\cos(3\phi_i)\ . \qquad (2.12)$$

The values of the coefficients in the bending and torsional potential models are summarized in Table 2.1. [18-20]

The last contribution to U^{intra} is the non-bonded dispersion interactions whose main purpose is to prevent unphysical overlaps between pseudo-atoms in the same molecule. In this work, Lennard-Jones is depicted in the figure 2.3, and it is treated as usual by pair-wise summation via a Lennard-Jones 12-6 potential,

$$U_{LJ}=4\varepsilon\left[\left(\frac{\sigma}{r}\right)^{12}-\left(\frac{\sigma}{r}\right)^{6}\right]\ . \qquad (2.13)$$

This treatment is also extended to the non-bonded pair interactions between pseudo-atoms (UA's) from different Pennzane molecules. The TraPPE force fields give appropriately different parameter values to the LJ potentials for different pseudo-atoms (UA's). These values are also summarized in Table 2.1. However, the same cutoff distance set at 14 Å is applied to all the LJ interaction pairs. [18-20]

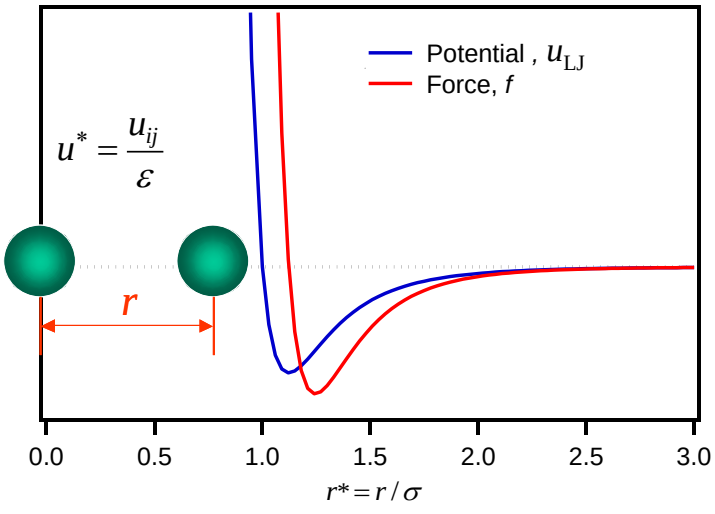

Figure 2.3. Lennard-Jones interaction potential as a function of inter-atomic distance.

Table 2.1. Values of the parameters in the intramolecular interaction potential models

Lennard-Jones Potential	group	CH_3	CH_2	CH
	σ[Å]	3.75	3.95	4.68
	$\varepsilon[k_B]$	98	46	10
Bond Bending	angle	CH_x-(CH_2)-CH_y	CH_x-(CH)-CH_y	cyclopentane
	θ_0 (deg)	114	112	105.5
Torsion	group	C-(CH_2)-(CH_2)-C	C-(CH_2)-(CH)-C	cyclopentane
	a_0	$1078.16k_B$	$507.09k_B$	$31394k_B$
	a_1	$355.03k_B$	$428.73k_B$	$45914k_B$
	a_2	$68.19k_B$	$111.85k_B$	$16518k_B$
	a_3	$791.32k_B$	$441.27k_B$	$1496k_B$

2.3. ALUMINA

Alumina can take on several different crystal structures, but the thermodynamically stable alumina phase and the most usual type found in nature is α-Al_2O_3. α-Al_2O_3 has a trigonal crystal structure [21] which can be illustrated by either a hexagonal or a rhombohedral lattice system. A hpc packing of spheres of oxygen atom is formed where alumina atoms account for two-third of the octahedral vacancies. Shown in Figure 2.4 is the conventional unit cell (hexagonal axes) of α-Al_2O_3 which contains 12 Al atoms and 18 O atoms, [21] corresponding to $Al_{12}O_{18}$. It should be noted here that Figure 2.4 includes 10 additional Al atoms (grey beads) and 4 additional O atoms (red beads) along the border axes in order to provide a clearer viewing. The unit cell can be

duplicated in all three directions to form a bulk phase of α-Al_2O_3. To form confining surfaces for the thing Pennzane film, the unit cell is only duplicated in the lateral directions in this work. The top-down (*xy*) and side (xz) views of the resultant α-alumina surface are shown in Figure 2.5.

Modeling Alumina Surface. Although a surface of rhombus shape is workable, it is computationally more efficient to simulate a model surface or a model system with square or rectangular shapes. For this purpose, four-unit cells can be combined together to identify a rectangular "computational unit cell", as indicated by the grey box in Figure 2.5(a), that contains 48 Al atoms and 72 O atoms, corresponding to $Al_{48}O_{72}$. This computation unit cell is 9.51 Å in length and 8.24 Å in width along the x and y directions, respectively, and is ready to be duplicated to construct a model alumina surface of any rectangular shape and any size. There has been a small number of MD modeling studies that involve the interactions between alkanes and alumina surface modeled [22,23] with an atomistic approach or a UA-like approach. In fact, these two approaches produce similar overall interactions between a psudo-atom and the Al_2O_3 surface. Since the UA approach has been employed for Pennzane, it is computationally sensible to also adopt the UA-like approach for modeling the interactions between Pennzane and the alumina surface. In this approach, the UA-O and UA-Al pair interactions are both modeled by the following modified LJ potential,

$$U = D_0 \left[\left(\frac{R_0}{r} \right)^{12} - 2 \left(\frac{R_0}{r} \right)^{6} \right] . \qquad (2.14)$$

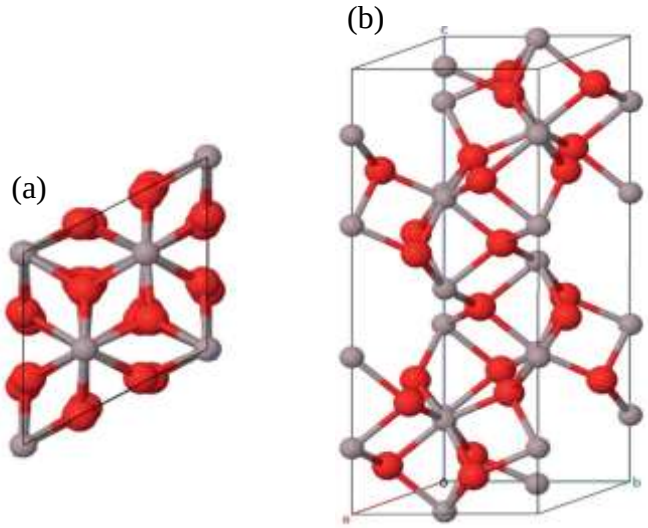

Figure 2.4. (a) Top-down view and (b) side view of the conventional hexagonal unit cell of α-Al_2O_3 where grey beads represent Al atoms while red beads denote O atoms.

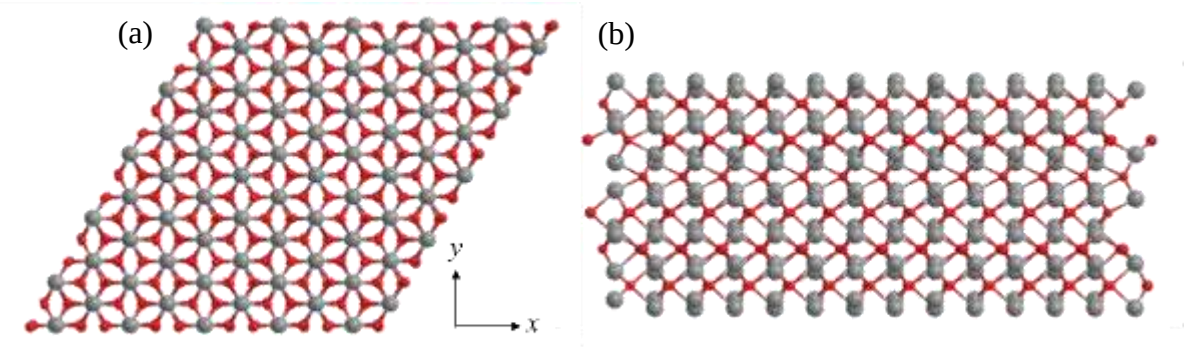

Figure 2.5. (a) Top-down (*xy*) view and (b) side (*xz*) view of the α-Al_2O_3 surface formed from duplicating the unit cell in the lateral directions.

The parameter values for different UA-Al(Al_2O_3) and UA-O(Al_2O_3) pair interactions are summarized in Table 2.2.

Table 2.2. Values of the parameters in the UA-Al(Al_2O_3) and UA-O(Al_2O_3) interaction potential models

Pair	CH_3-Al	CH_3-O	CH_2-Al	CH_2-O	CH-Al	CH-O
R_0 [Å]	4.286	3.878	4.296	3.880	4.296	3.880
D_0 [J/mol]	1125.496	348.946	932.614	291.645	932.614	291.645

2.4. INITIAL CONDITION

The initial coordinates of the pseudo-atoms in a single Pennzane molecule were first adopted from the [24] PubChem database. The molecule was then duplicated once and carefully placed next to the first one at such a distance that their UA's have only attractive interactions without any repulsion. Afterwards, the same procedure was employed to duplicate Pennzane dimer and higher oligomers multiple times to arrive at a thin film that contains 30 Pennzane molecules. This film was then duplicated and stacked on one another to achieve an initial condition, as shown in Figure 2.6, that contains 60 Pennzane molecules comprising 3900 UA's.

To complete the construction of the initial condition for the subsequent MD simulations, the computational unit cell discussed above was duplicated 11×11 times and arranged together to have a model Al_2O_3 surface whose lateral (*xy*) dimensions are 104.65 Å×90.63 Å and which contains 5808 Al atoms and 8712 O atoms. This surface was then duplicated again and placed together to sandwich the initial Pennzane film

obtained above. The initial separation between the two confining alumina surfaces based on their topmost Al atoms is set at $h = 42.69$ Å. This surface separation allows the Pennzane molecules to have attractive interactions with the surfaces but without any unphysical repulsion. A side view of the completed initial condition is shown in Figure 2.7. It is worth emphasizing here that periodic boundary conditions [15,16] were always applied in the lateral (*xy*) directions in this work.

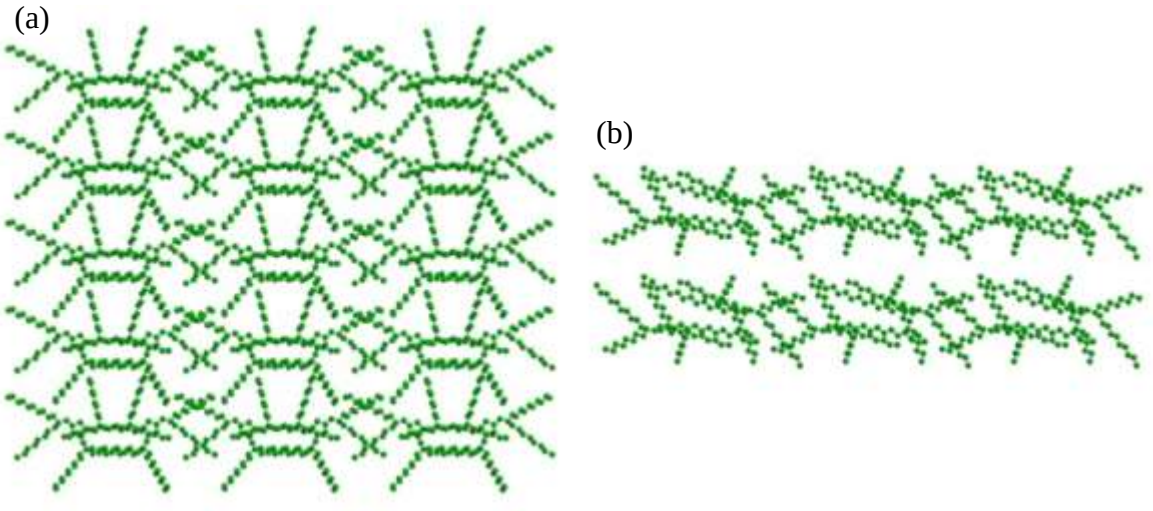

Figure 2.6. (a) Top-down (*xy*) view and (b) side (*xz*) view of the initial Pennzane film that contains 60 Pennzane molecules (3900 UA's).

Regardless of how carefully prepared an initial condition was, it is still full of artificial information that may significantly and negatively affect the results and analyses to be generated from MD simulations. It is necessary to allow the initial condition to evolve toward a thermodynamically consistent state. This equilibration procedure started from a very small time interval, $\Delta t = 0.3$ fs, in this work and gradually increased the time interval to 1.5 fs over several million time steps totaling more than 3.5 ns (10^{-9} sec),

during which the system temperature is controlled at 25 ℃ (298.15 K) and the separation between the confining alumina surfaces is kept at $h = 42.69$ Å.

Although the exact definition of the volume of a nanoscopically confined space is lacking, it is reasonable to approximate it as the product of the lateral dimensions and a 'free' separation that is equal to $\left(h - 2R_{0,\mathrm{CH_2\text{-}Al}}\right)$. Based on this approximation, the volume space of the initial condition is 3.234×10^{-19} cm^3, resulting in a Pennzane film density of ~0.304 g/cm^3. It can be expected that under high load conditions, the film density would increase in order to support the applied loads. To study such conditions in MD simulations, different equilibrated systems with decreased film thicknesses (surface separations) are needed. For this purpose, the initial equilibrated system was subjected to a slow, stepwise process to gradually decrease the surface separation over several million time steps. The new equilibrated system has a separation of $h = 27.45$ Å, corresponding to an approximate film density of ~0.0.549 g/cm^3.

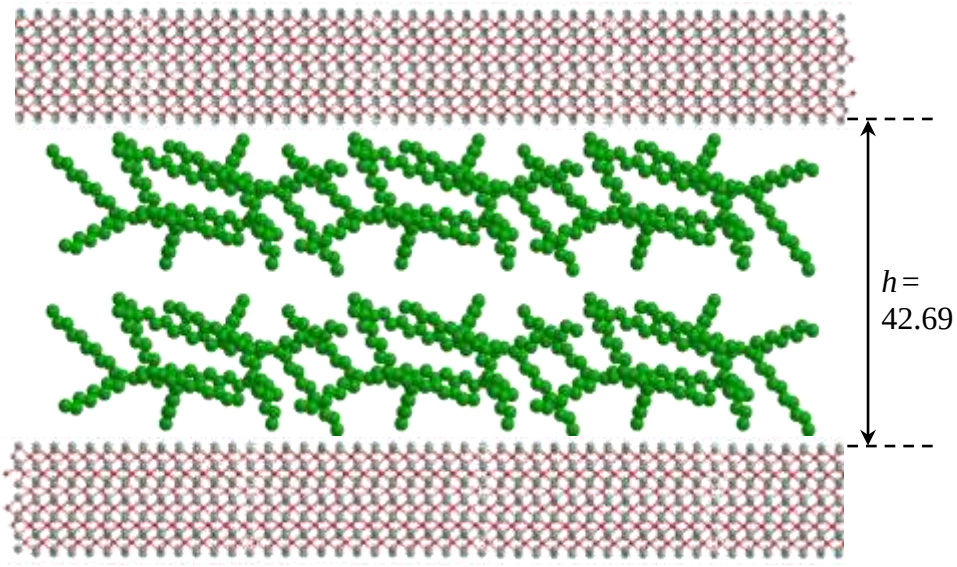

Figure 2.7. Side (*xz*) view of the initial condition

3. RESULTS AND ANALYSIS

3.1. CONFIGURATIONS OF PENNZANE THIN FILM

To the best of our knowledge, Pennzane thin film confined between two solid surfaces appears to have not received much research effort in terms of theoretical or MD modeling studies. To date, we have found only one publication that reported complementary experimental and MD studies involving a confined Pennzane thin film[26]. However, its focus was to investigate the effects of two lubricant additives and very little was reported concerning Pennzane or the details of the simulation potentials. In fact, it appeared to involve a very small number of Pennzane molecules in a very finite system sandwiched by two simple generic surfaces. From a fundamental and modeling perspective, such a model system is likely to be subject to very significant "finite-size" effects [15].

In this work, two equilibrated systems were considered and compared with one another. Case A has a larger surface separation (42.69 Å) and hence a lower film density, whereas case B has a smaller surface separation (27.45 Å) and hence a higher film density. The simulation results and subsequent analyses were based on production runs spanning 300 ps. Shown in Figures 3.1 and 3.2 are the simulation snapshots of the two systems before and after the production runs. Compared to symmetric molecules in similar nano-scale confinement which tend to form layers parallel to the confining surfaces [26-30], thereby exhibiting solid-like yield stress and stick-slip motion instead of lubricated smooth motion, Pennzane does not appear to be layered to any significant extent, which can be attributed to its highly branched and highly asymmetric structure

[28-30]. Moreover, comparison between the simulation snapshots before and after the production runs indicates that Pennzane molecules in the confined space still retain substantial mobility in both cases as their positional changes are very noticeable during the span of 300 ps. Such a high mobility could be related to the non-layered configurations and could have very significant implications to the tribological behavior of thin Pennzane lubricant film for space and nanotechnological applications.

It is also apparent from the snapshots that stretched conformations are retained in many of the branches of the Pennzane molecules adjacent to the alumina surfaces adopt

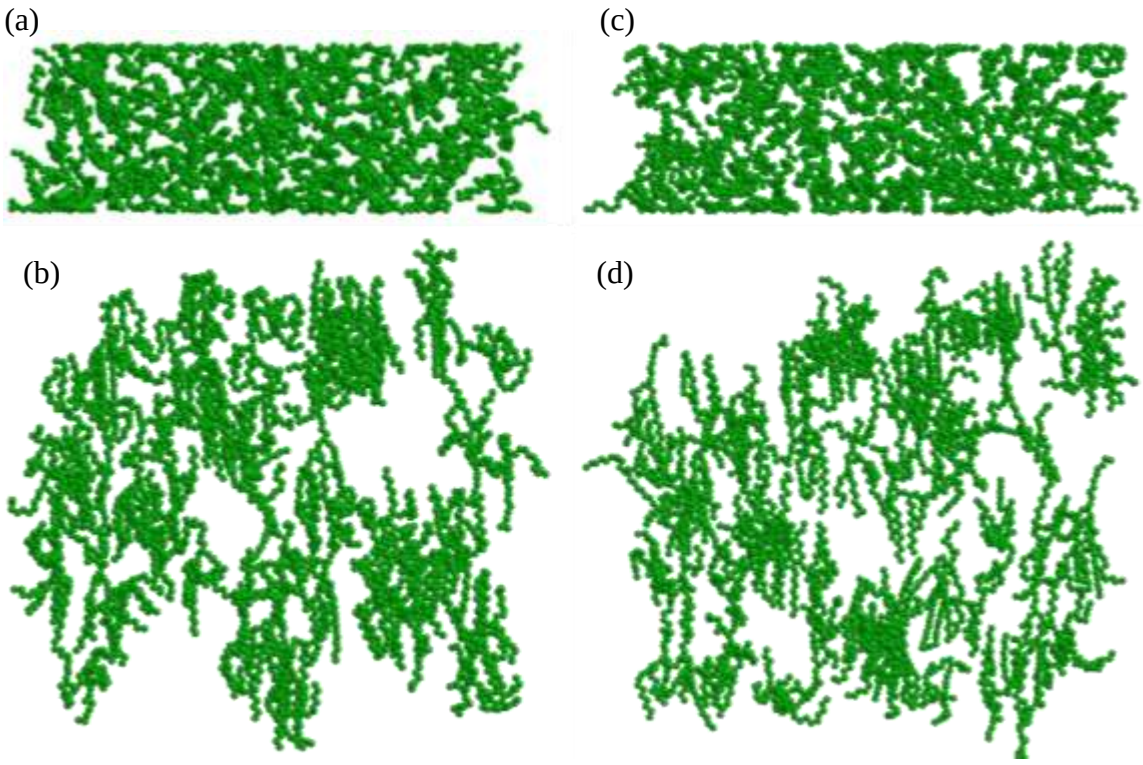

Figure 3.1. Simulation snapshots of Pennzane films in case A before (left panel) and after (right panel) the production run. (a) and (c) are side (*xz*) views, while (b) and (d) are top-down (*xy*) views.

stretched conformations and lie parallel to the surfaces. Those branches in direct contact with the surfaces appear to have segments lying parallel on the surfaces. These conformations and orientation are made possible due to Pennzane's sufficient structural flexibility and natural tendency to maximize interactions with the surfaces.

3.2. DENSITY DISTRIBUTIONS IN PENNZANE THIN FILM

The simulation snapshots only provide the configurations and conformations at certain time instant. Judging by their significant mobility, Pennzane molecules can be expected to exhibit fairly uniform distributions in the lateral directions over a sufficiently large time scale. Shown in Figure 3.3 are the time-averaged lateral distributions of Pennzane pseudo-atoms (UA's) for both cases, which are consistent with expectation.

In the confining (z) direction, however, non-uniform distributions are expected as they were also hinted by the side views in Figures 3.1 and 3.2. For quantitative analysis, the time-averaged density distributions of the Pennzane pseudo-atoms and centers of mass are computationally determined and plotted in Figures 3.3, 3.4 and 3.5 respectively. These density distributions do possess persistent oscillatory patterns, but they are far from being layered configurations as those seen in symmetric molecules [28-30]. These oscillatory density patterns will not be averaged out even if much longer time periods are employed as it is a persistent effect imparted by the nanoscopic confinement [26-30]. Notably, the nature of the confining surfaces may affect the magnitude of the oscillations but cannot make the oscillations disappear. However, the nature of the confining surfaces does affect the density of the adjacent molecules. Since there are attractive interactions from the alumina surfaces, the Pennzane molecules exhibit

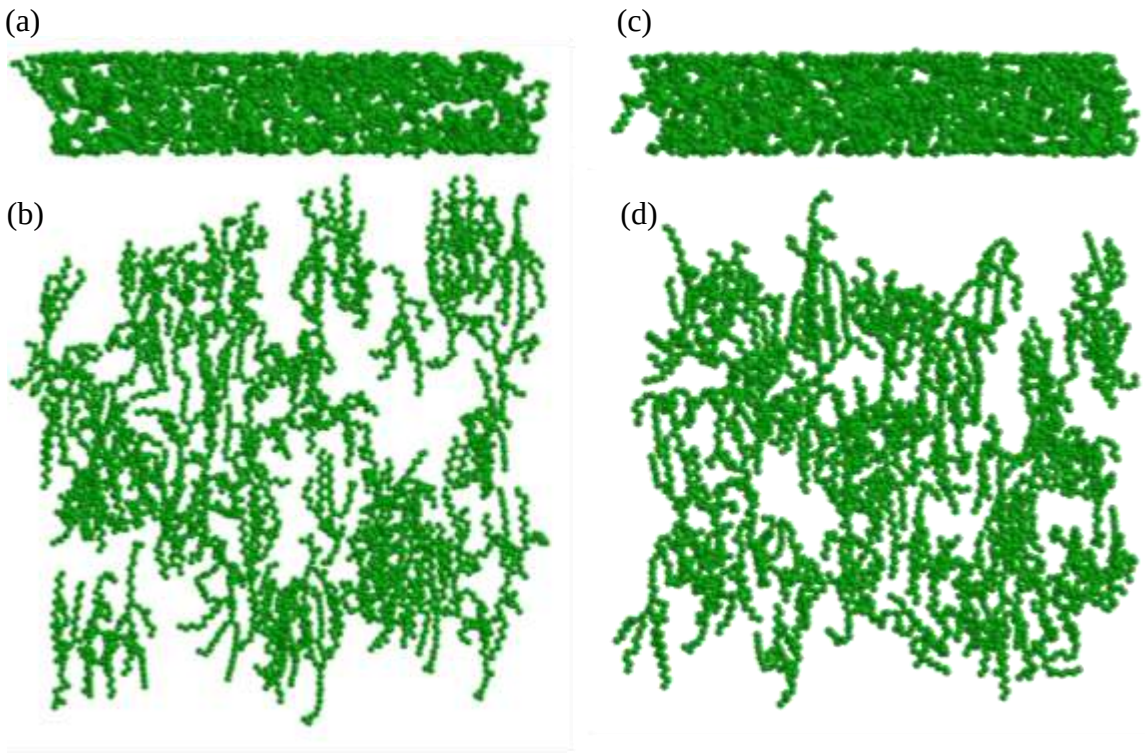

Figure 3.2. Simulation snapshots of Pennzane films in case B before (left panel) and after (right panel) the production run. (a) and (c) are side (*xz*) views, while (b) and (d) are top-down (*xy*) views.

enhanced UA and center-of-mass densities adjacent to the surfaces, which were also observed in the simulation snapshots presented in Figures 3.1 and 3.2.

3.3. ALKYL BRANCHES IN PENNZANE THIN FILM

The long alkyl branches are the predominant structural feature of Pennzane molecule and can be understood to be responsible for many interesting and important properties possessed by Pennzane. It is of great interest and importance to investigate how the long branches are accommodated in the confined space.

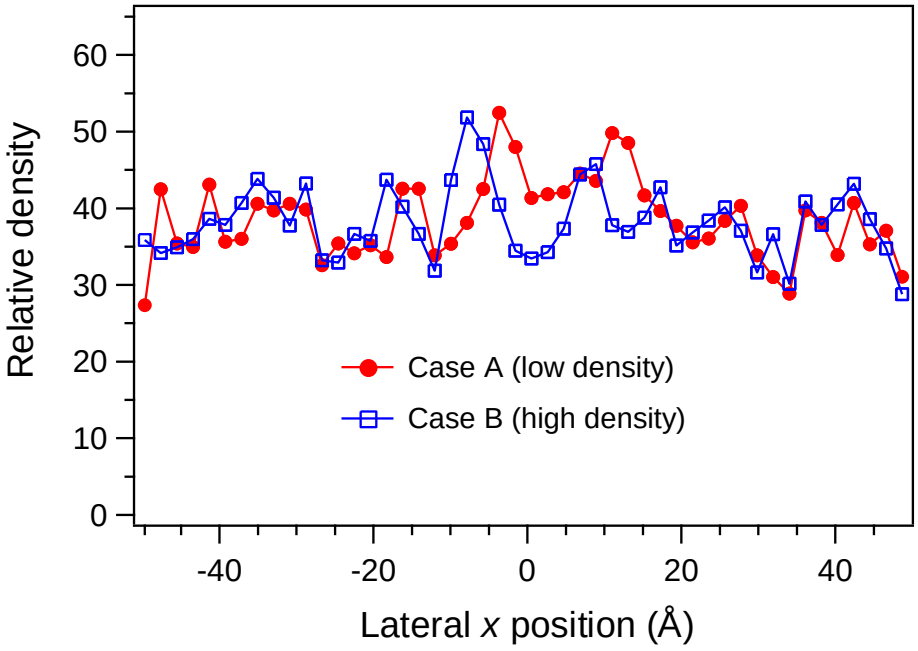

Figure 3.3. Time-averaged density distributions of Pennzane pseudo-atoms (UA's) in a lateral direction.

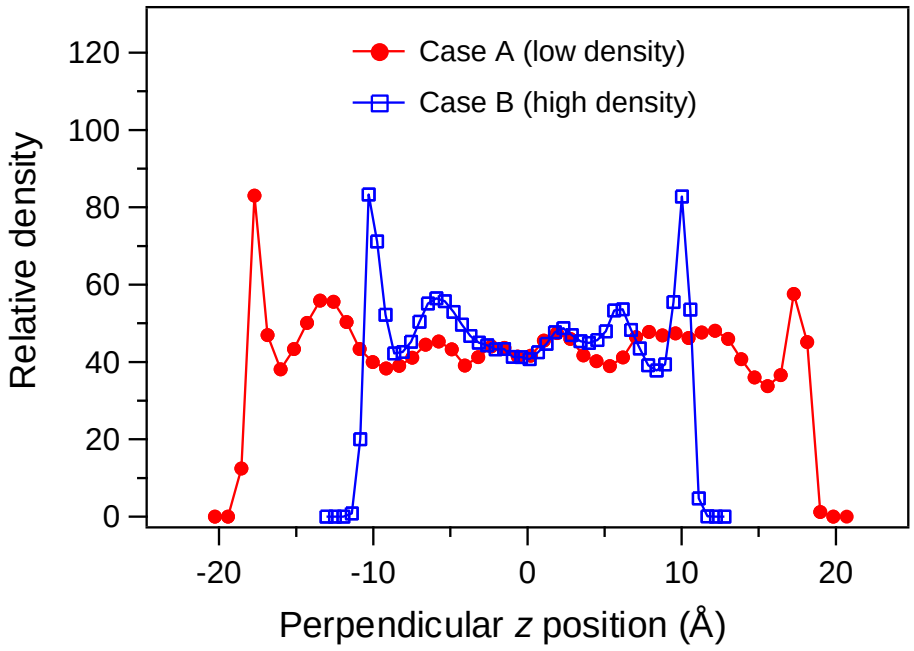

Figure 3.4. Time-averaged density distributions of Pennzane pseudo-atoms (UA's) in the confined direction.

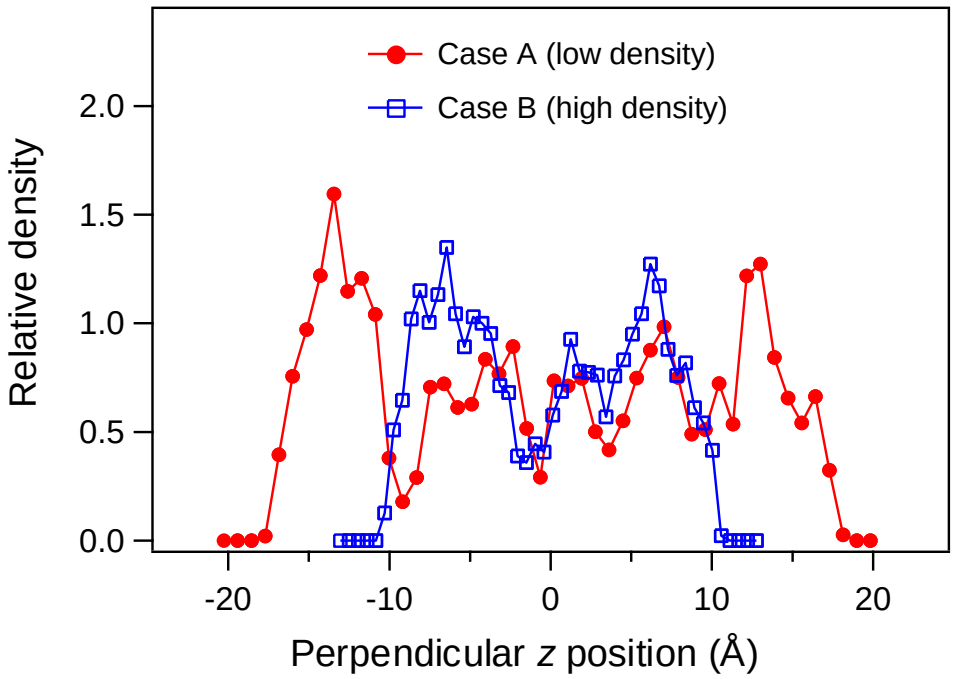

Figure 3.5. Time-averaged density distributions of Pennzane centers of mass in the confined direction.

Insights in this respect could be revealed by the distributions of branch length and branch orientation in the perpendicular z direction. For this purpose, the geometric center of the core cyclopentane was taken as the reference and the positions of the six terminal UA's (labeled 9, 27, 28, 46, 47, 65 in Figure 2.2) were used to evaluate branch length and branch orientation. In this manner, the C_8 and C_{10} branches in an ideal, fully stretched pennzane molecule (e.g., Figure 2.2) are 12.3 Å and 16.5 Å in length, respectively. From Figure 3.6 where the branch length was shown as a function of terminal UA's position in the perpendicular *z* direction, the branch length can be seen to be shorter than 14.4 Å, the average length of fully stretched C_8 and C_{10} branches, meaning that the structural flexibility has allowed non-trans conformations to take place and to remain. It can also be seen from the figure that strong interactions from the surfaces can assist structural

flexibility to allow higher degrees of non-trans conformations and shorter branch lengths in Pennzane molecules in the immediate proximity of the surfaces. However, there could be a number of different ways for this trend to take place.

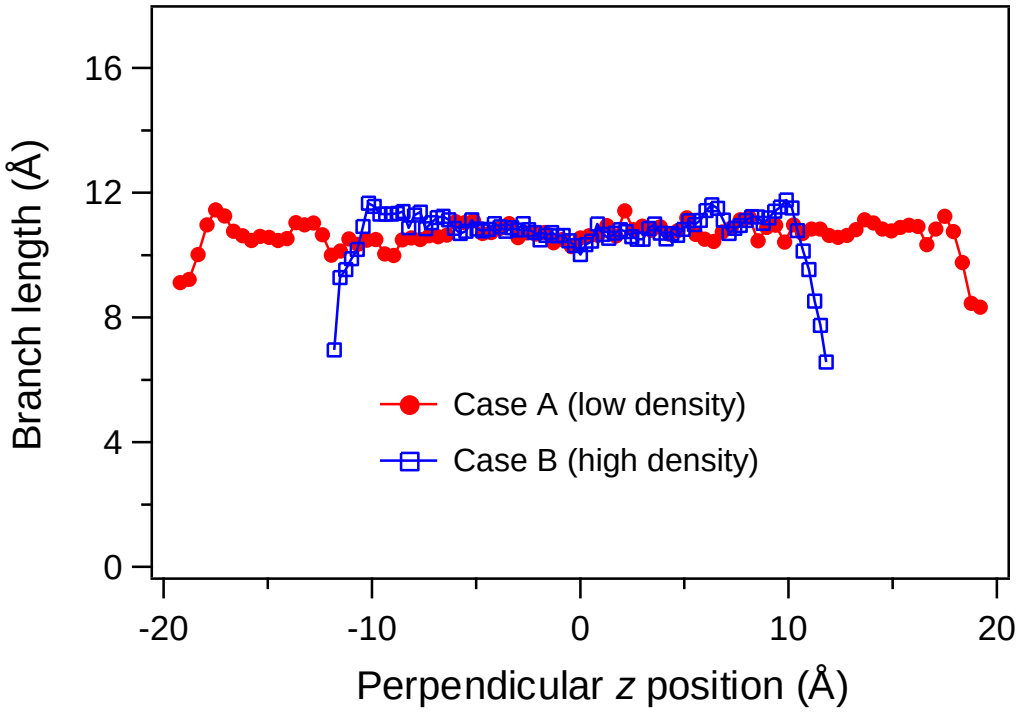

Figure 3.6. Distribution of branch length as a function of terminal UA's position in the confined direction.

Using the same reference, the end-to-center vectors can be determined using the six terminal UA's positions in each Pennzane molecule. These vectors can then be used to determine the angles of the branches with respect to the perpendicular (z) direction. The results from the MD simulations are presented in Figure 3.7. Interestingly, the branches mostly fall within a narrow range of angles around 52° except when they are right next to the surfaces where decreased branch angles coincide with decreased branch lengths. This means that the alkyl branches in direct interaction contact with the alumina

surfaces tend to stand more perpendicularly to the surfaces than those away from. This phenomenon is similar to the chain orientations in self-assembled monolayers (SAMs) which require strong surface interactions and high chain densities [22].

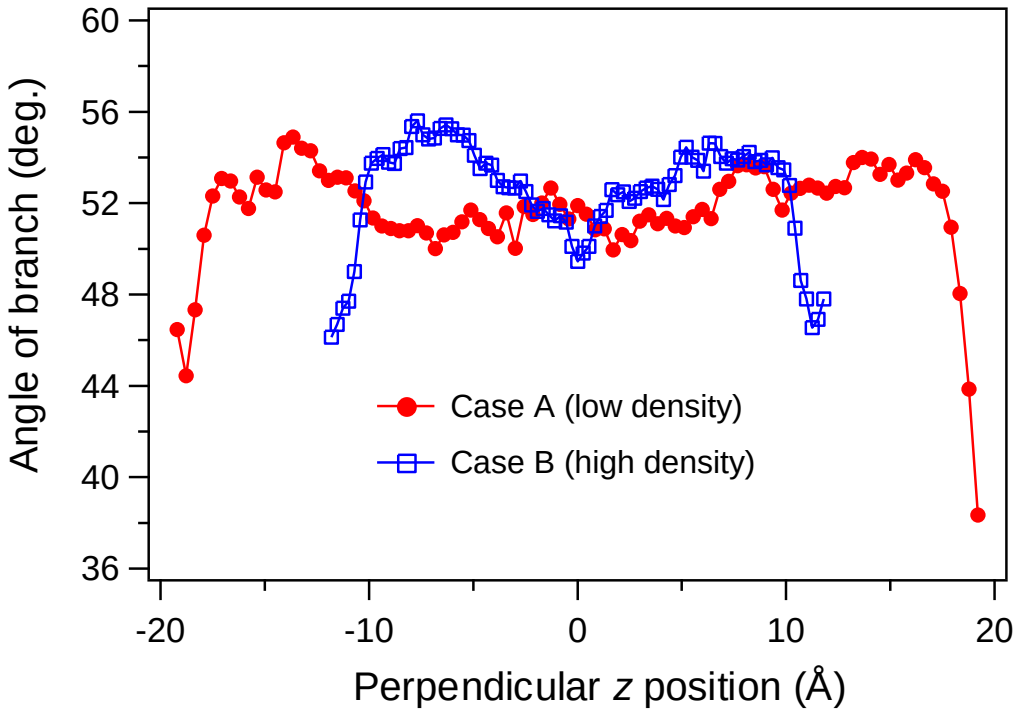

Figure 3.7. Distribution of branch angle as a function of terminal UA's position in the confined direction.

3.4. CONCLUSIONS

Pennzane is a highly branched synthetic hydrocarbon that has been shown to outperform many traditional lubricants. It has been increasingly utilized for be in space engineering and other emerging applications. However, our recognition of Pennzane being an excellent lubricant relies mostly on experimental measurements and indirectly

on inference from theoretical studies of other molecules. Fundamental insights and understanding are still needed in order to understand the full potential as well as the limitation of Pennzane. To this end, molecular dynamics (MD) is a very well-suited method but has virtually not been applied to the study of Pennzane to this date. In this work, appropriate potential models were identified and utilized for simulating Pennzane molecules. The MD simulation codes were successfully developed, and realistic model systems were constructed comprising Pennzane thin films sandwiched between two confining surfaces. To make the model systems more relevant practically, α-alumina surfaces were considered and atomistically represented in the MD simulations.

The results from the MD simulations in this work show that, unlike symmetric molecules that can be induced by nanoscopic confinement to form layered configurations, the highly branched Pennzane possesses sufficient structural asymmetry and complexity to resist the layering tendency, which can be linked to its exceptional tribological properties. In addition, confined Pennzane retains high mobility, which is less solid-like and hence more likely to provide reduced friction and wear. In addition, Pennzane thin films have more uniform density distributions across surface separation, meaning that they are more efficient in transferring momentum and possibly heat as well. Detailed analyses of the lengths and angles of the Pennzane branches show that, in general, the branches are able to maintain similar lengths and angles throughout the confined thin films except the regions in direct contact with strongly interacting surfaces. More specifically, strong interactions from the surfaces, assisted by the structural flexibility of the Pennzane branches, are able to bend segments of the proximal branches into non-trans conformations that lie directly on and parallel to the surfaces. The resultant strong

interactions appear to function as an anchor that promotes the branches in a crowded environment to stand more straight up, a phenomenon similar to self-assembled monolayers (SAMs).

The realistic model system of an important liquid lubricant developed in this work can be considered to be equivalent to a key that can open many research directions and opportunities. It will enable the effects of inorganic lubricant additives such as graphene and organic lubricant additives such as tri-(2-octyldodecyl) phosphate to be studied in the near future by MD simulations. It can also be integrated with other components in MD simulations to explore nanotechnological applications.

BIBLIOGRAPHY

1. William R. Jones Jr. and Mark J. Jansen, "NASA/TM- 2000-209924 Space tribology", Pg. 1-20, March 2000.

2. Clifford Venier, William R. Jones, et al., "Tribological properties of pennzane based lubricant for low temperature space applications", *Proceedings of 36th Aerospace Mechanisms Symposium*, pp. 331-338, 2002.

3. P.D. Fleischauer and M.R. Hilton, "Assessment of the Tribological Requirements of Advanced Spacecraft Mechanisms", Report TOF0090 (5064)-1, Aerospace Corporation, El Segundo, California, 1991.

4. https://www.nyelubricants.com/pennzane. Nye Lubricants- pennzane™ lubricant, July 2019.

5. Ping Yang, Huazhong Zhang, "Numerical analysis on meshing friction characteristics of nano-gear tear", *Tribology International*, pp 535-541, 2008.

6. Mario Marchettia, William R. Jones, Jr., et al, "Tribological Performance of Some Pennzane Based Greases for Vacuum Applications", *Tribology Letters NASA*, Vol. 12, Pg. 202-216, May 2002.

7. Diana Berman, Ali Erdemir, Anirudha V., "Graphene: A New Emerging Lubricant, Materials Today", *American Chemical Society*, Vol. 17, Pg. 31-42, 2014.

8. K. S. Novoselov, D. Jiang, et al, "Two-dimensional Atomic Crystals", *Proceedings of the National Academy of Science*, 10451-10453, 2005.

9. C. Lee et al, "Frictional Characters of Atomically Thin Sheets", *AAAS Science*, Pg. 76 – 80, 2010.

10. G. H. Lee et al, "High Strength Chemical Vapor Deposited Graphene and Grain Boundaries", *AAAS Science*, Pg. 1073-1076, 2013.

11. S. S. Kandanur, MA Rafiee, et al., "Suppression of Wear in Graphene-Polymer Composites", Vol 50, *Journal of Carbon*, Pg. 3178-3183, 2012.

12. E. Singh, R. Mukharjee, et al, "Graphene Drape Minimizes the Pinning and Hysteresis of Water Drops on Nanotextured Rough Surfaces", *American Chemical Society*, Pg 3512-3521, 2013.

13. Z. Rymuza, "Anti Wear Coatings" in *Tribology of Miniature Systems*, Elsevier, pp. 288-300, 1989.

14. http://www.madehow.com/Volume-6/Gyroscope.html. How Gyroscopes are made. July 2019

15. M. P. Allen and D. J. Tildesley, "*Computer Simulation of Liquids*", Clarendon Press: Oxford, U.K., 1987.

16. D. Frenkel and B. Smit, "*Understanding Molecular Simulation: From Algorithms to Applications*", Academic Press: New York, 2001.

17. D. Brown and J. H. R. Clarke, "A Comparison of Constant Energy, Constant Temperature and Constant Pressure Ensembles In Molecular Dynamics Simulations Of Atomic Liquids". *Molecular Physics*, Vol. 51, pp. 1243-1252, 1984.

18. M. G. Martin and J. I. Siepmann, "Transferable Potentials for Phase Equilibria. United-Atom Description of *N*-Alkanes", *Journal of Physical Chemistry B*, Vol. 102, pp. 2569-2577, 1998.

19. M. G. Martin and J. I. Siepmann, "Novel Configurational-Bias Monte Carlo Method for Branched Molecules. Transferable Potentials for Phase Equilibria, United-Atom Description Of Branched Alkanes", *Journal of Physical Chemistry B*, Vol. 103, pp. 4508-4517, 1999.

20. S. J. Keasler, S. M. Charan, C. D. Wick, I. G. Economou, and J. I. Siepmann, "Transferable Potentials for Phase Equilibria−United Atom Description of Five- and Six-Membered Cyclic Alkanes and Ethers", *Journal of Physical Chemistry B*, Vol. 116, pp. 11234−11246, 2012.

21. M. F. Peintinger, M. J. Kratz, and T. Bredow, "Quantum-Chemical Study Of Stable, Meta-Stable and High-Pressure Alumina Polymorphs and Aluminum Hydroxides", *Journal of Materials Chemistry A*, Vol. 2, pp. 13143-13158, 2014.

22. C. Li and P. Choi, "Molecular Dynamics Study of The Adsorption Behavior Of Normal Alkanes on a Relaxed α-Al_2O_3 (0001) Surface", *Journal of Physical Chemistry C*, Vol. 111, pp. 1747-1753, 2007.

23. P. de Sainte Claire, K. C. Hass, W. F. Schneider, and W. L. Hase, "Simulations of Hydrocarbon Adsorption and Subsequent Water Penetration on an Aluminum Oxide Surface", Journal of Chemical Physics, Vol. 106, pp. 7331-7342 , 1997.

24. https://pubchem.ncbi.nlm.nih.gov/. National Center for Biotechnology Information. PubChem Compound Database.

25. J. Nian, Y. Si, Z. Guo, P. Gao, W. Liu, “Characterizing a lubricant additive for 1,3,4-tri-(2-octyldodecyl) cyclopentane: Computational study and experimental verification, *Friction*, Vol. 4, pp. 257-265, 2016.

26. H.-W. Hu, G. A. Carson, and S. Granick, “Relaxation time of confined liquids under shear”, *Physical Review Letter*, Vol. 66, pp. 2758-2761, 1991.

27. H. Yoshizawa and J. N. Israelachvili, “Fundamental mechanisms of interfacial friction. 2. Stick-slip friction of spherical and chain molecules”, *Journal of Physical Chemistry*, Vol. 97, pp. 11300-11313, 1993.

28. J.-C. Wang and K. A. Fichthorn, “Molecular Dynamics Studies of the Effects of Chain Branching on the Properties of Confined Alkanes”, *Journal of Chemical Physics*, Vol. 116, pp. 410-417, 2002.

29. J.-C. Wang and K. A. Fichthorn, “Influence of Molecular Structure on the Properties of Confined Fluids by Molecular-Dynamics Simulation”, *Colloids and Surfaces A: Physicochemical and Engineering Aspects*, Vol. 206, pp. 267-276, 2002.

30. J.-C. Wang and S. Saroja, “Modeling Confined Fluids: an *NhPT* Method”, *Molecular Simulation*, Vol. 29, pp. 495-508, 2003.

31. A. Ulman, “Self-assembled monolayers of alkyltrichiorosilanes: Building blocks for future organic materials”, *Advanced Materials*, Vol. 2, pp. 573-582, 1990.

32. J. C. Love, L. A. Estroff, J. K. Kriebel, R. G. Nuzzo, G. M. Whitesides, “Self-assembled monolayers of Tthiolates on metals as a form of nanotechnology”, *Chemical Reviews*, Vol. 105, pp. 1103-1170, 2005.

VITA

Vidit Singh was born in Ranchi, India. He received his bachelor's degree in chemical engineering from National Institute of Technology, Raipur, Chhattisgarh, India. After graduation, Vidit worked as Process Engineer in Heidelberg Cement India Pvt Ltd., Madhya Pradesh, India from July 2015 – October 2016. He started at Missouri University of Science and Technology, Rolla, during the fall semester of 2017 to work under the supervision of Dr. Jee-Ching Wang. He received the Master of Science degree in Chemical Engineering from Missouri University of Science and Technology in December 2019.